(20) Becker, E. D. *High Resolution NMR*; Academic: New York, 1980.
(21) Davis, J. H.; Jeffrey K. R.; Bloom, M.; Valic, M. I.; Higgs, T. P. *Chem. Phys. Lett.* **1976**, *42*, 390.
(22) Blinc, R.; Rutar, V.; Seliger, J.; Slak, J.; Smolej, V. *Chem. Phys. Lett.* **1977**, *48*, 576.
(23) Hentschel, R.; Spiess, H. W. *J. Magn. Reson.* **1979**, *35*, 157.
(24) Batchelder, L. S.; Niu, C. H.; Torchia, D. A. *J. Am. Chem. Soc.* **1983**, *105*, 2228.
(25) Torchia, D. A. *Annu. Rev. Biophys. Bioeng.* **1984**, *13*, 125.
(26) Jelinski, L. W., unpublished data.
(27) Spiess, H. W.; Sillescu, H. *J. Magn. Reson.* **1981**, *42*, 381.
(28) Inglefield, P. T.; Jones, A. A.; Lubianez, R. P.; O'Gara, J. F. *Macromolecules* **1981**, *14*, 288.
(29) Jones, A. A.; O'Gara, J. F.; Inglefield, P. T.; Bendler, J. T.; Yee, A. F.; Ngai, K. L. *Macromolecules* **1983**, *16*, 658.
(30) Inglefield, P. T.; Amici, R. M.; O'Gara, J. F.; Hung, C.-C.; Jones, A. A. *Macromolecules* **1983**, *16*, 1552.
(31) Schaefer, J.; Stejskal, E. O.; McKay, R. A.; Dixon, W. T. *Macromolecules* **1984**, *17*, 1479.
(32) Garroway, A. N.; Ritchey, W. M.; Moniz, W. B. *Macromolecules* **1982**, *15*, 1051.
(33) Gupta, M. K.; Ripmeester, J. A.; Carlsson, D. J.; Wiles, D. M. *J. Polym. Sci., Polym. Lett. Ed.* **1983**, *21*, 211.
(34) Petrie, S. E. B.; Moore, R. S.; Flick, J. R. *J. Appl. Phys.* **1972**, *43*, 4318.
(35) Jelinski, L. W.; Dumais, J. J.; Cholli, A. L. *Polym. Prepr. (Am. Chem. Soc., Div. Polym. Chem.)* **1984**, *25*(1), 348.

Characterization of Polymer Blends by Selective Proton Spin-Diffusion Nuclear Magnetic Resonance Measurements

P. Caravatti,[†] P. Neuenschwander,[‡] and R. R Ernst*[†]

Laboratorium für Physikalische Chemie and Institut für Polymere, Eidgenössische Technische Hochschule, 8092 Zürich, Switzerland. *Received January 21, 1986; Revised Manuscript Received May 1, 1986*

ABSTRACT: Spin diffusion in proton nuclear magnetic resonance has been used to study binary blends of polystyrene and poly(vinyl methyl ether). By means of a selective excitation technique, it was possible to detect the coexistence of pure and mixed domains. Within the framework of a simple three-phase model, the total amount of polymer contained in the mixed phase and its composition could be determined.

I. Introduction

The blending of polymers offers the possibility of tailoring new technically important materials with specified physical properties.[1-3] Only a small number of polymer combinations leads to thermodynamically stable blends. In most cases the artificially enforced mixtures are far from thermodynamic equilibrium and unstable. Because of low translational mobility in macromolecular systems, equilibration may proceed very slowly. The distinction between compatible and incompatible blends is in many cases not trivial. It is therefore of importance to have available analytical tools for studying phase separation on a microscopic scale. Several techniques have been applied so far, in particular, diffraction methods,[4-8] thermal analysis,[9] and electron microscopy.[10] Compatible blends exhibit a single glass transition temperature T_g while for incompatible blends the glass transitions of the individual homopolymer components can be detected. Standard methods for the determination of T_g are differential scanning calorimetry (DSC),[11,12,27] dilatometry,[13] dynamic mechanical relaxation,[14,15] and dielectric relaxation measurements.[16,17] It has also been recognized by several researchers that spin diffusion in nuclear magnetic resonance can provide information on heterogeneity.[18-25]

In a recent study, two-dimensional (2D) NMR spectroscopy was used for obtaining revealing plots that qualitatively allow the distinction between compatible and incompatible mixtures.[26] To describe a binary mixture of two distinct polymers, a three-phase model has been proposed with two pure polymer phases and a mixed phase. By 2D spin-diffusion measurements, it was possible to deduce bounds for the composition of the mixed phase. However, it turned out to be a priori impossible to determine the exact composition of the mixed phase by 2D or by transient 1D measurements.

It will be demonstrated in this paper that one-dimensional (1D) saturation-transfer experiments allow immediate access to the composition of the mixed phase. Transient spin-diffusion measurements can be used for the determination of spin-diffusion rate constants, which provide information on the size of the domains and on molecular mobility. The measurements reported here focus on proton spin diffusion, which is particularly informative as it proceeds at a high rate and is not much impeded by competing relaxation processes.

II. Samples

Binary polymer blends consisting of atactic polystyrene (PS) (supplied by BASF) and atactic poly(vinyl methyl ether) (PVME) (Aldrich-Chemie, Steinheim, BRD) were used. Both polymers have a distribution of molecular weights. The sample of PS is characterized by $\bar{M}_\eta = 279\,000$ (toluene, 25 °C) and $\bar{M}_w/\bar{M}_n = 2.5$ and the sample of PVME by $\bar{M}_\eta = 53\,500$ (benzene, 30 °C) and $\bar{M}_w/\bar{M}_n \simeq 2.0$ as estimated from gel permeation chromatography (GPC) measurements. The blending was effected by precipitation from a homogeneous solution of the two polymers in toluene or chloroform (containing 2.5% of each polymer) by adding a large excess of petroleum ether cooled to −60 °C. The precipitate was filtered off and vacuum dried for 48 h at room temperature. Samples of 50 mg were necessary for the NMR measurements.

It is well-known from thermal analysis[27,28] and from proton NMR relaxation studies[29] that the physical properties of this particular blend depends on the solvent from which it is precipitated. Some indication of this behavior could already be deduced by visual inspection of the two blends. The blend cast from toluene (B_T) appeared more transparent than the blend cast from chloroform (B_C). The blend B_T remained unaltered even after storing for 6 months at room temperature while the blend

[†] Laboratorium für Physikalische Chemie.
[‡] Institut für Polymere.

0024-9297/86/2219-1889$01.50/0

B_C showed a macroscopic phase separation that slowly developed in the course of this period.

III. Measurement Techniques

The two experimental techniques used in this work have been described and analyzed in detail in a separate more technical report.[37] In this section we give only a brief summary of the main features.

Nuclear spin diffusion is driven by the magnetic dipolar interaction of nuclear spins which can induce mutual flips of two spins j and k at a rate R_{SD} proportional to the inverse sixth power of their internuclear separation r_{jk}.[30] Based on this strong distance dependence, it is possible to derive information on spatial proximity in solid materials. In general, spin diffusion between two molecular species can only be detected when the two species are mixed on a molecular level.

Although the dipolar interactions are of short range, the magnetization can migrate in a diffusion-like process over quite significant distances within extended networks of interacting spins. From the analysis of spatial spin diffusion it is possible to detect different phases in inhomogeneous polymer systems to compute their composition and to estimate the size of small domains.

A spin-diffusion experiment can generally be divided into three time intervals: (i) the initial labeling of the spin order, (ii) the actual spin-diffusion process, and (iii) the detection process. While in earlier measurements[31-33] differences in relaxation times T_2 or $T_{1\rho}$ have been exploited to distinguish the components, our measurements rely on direct spectral resolution of the different components in the polymer blend. The initial labeling of the spin order is then achieved by free precession of the spins during the t_1 period in a 2D experiment[26] or by a frequency-selective inversion of the polarization of one component.

For obtaining sufficient resolution in proton magnetic resonance, both for the selective inversion and the detection, it is mandatory to eliminate temporarily the dipolar interactions as well as the chemical shielding anisotropy. Dipolar interactions are rendered ineffective by applying a multiple-pulse sequence, such as the MREV-8 cycle, while the chemical shielding anisotropy is eliminated simultaneously by magic-angle sample spinning at a rate of 2 to 3 kHz.[34-36]

A special procedure had to be developed for the selective irradiation in the presence of multiple pulse dipolar decoupling, a prerequisite for the following two techniques. Details are given in ref 37.

(a) Selective Inversion–Recovery Experiment. The selective inversion–recovery experiment serves for the measurement of the spin-diffusion rate constants. The experimental scheme shown in Figure 1a has its analogy in corresponding methods used in liquid-state NMR[38-44] and in solid-state ^{13}C resonance[45] for the study of cross-relaxation and chemical exchange.

Initially, a selective π pulse inverts the polarization of one isochronous group of spins. Its diffusion to other groups of spins in the course of the mixing time τ_m is monitored by applying a nonselective $\pi/2$ pulse followed by a sequence of MREV-8 multiple-pulse cycles[46,47] for achieving high resolution during detection. The experiment is repeated for several τ_m values.

Some further modifications are needed to suppress possible artifacts. To prevent leakage of spurious transverse magnetization into the detection period, due to the possibly not fully perfect selective inversion pulse, two experiments have to be coadded, differing by a π phase shift of the selective pulse. An equivalent and, for experimental reasons, sometimes superior procedure is to introduce in one of the two experiments to be coadded, a π_z pulse immediately following the selective pulse, as indicated in Figure 1a. In addition, it is advisable to phase-alternate the detection pulse together with the computer phase to eliminate artifacts originating from the multiple-pulse sequence during detection. Each experiment thus consists of four scans.

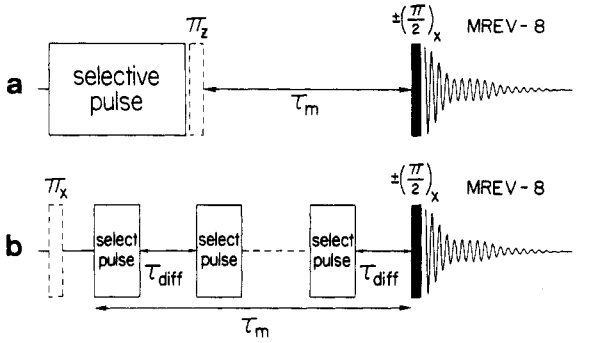

Figure 1. Pulse sequences for selective spin diffusion measurements. (a) Selective inversion–recovery experiment. A selective π pulse inverts a single line, narrowed by simultaneous homonuclear multiple pulse dipolar decoupling. After spin diffusion for a time τ_m, the full spectrum is excited by a nonselective $\pi/2$ pulse and measured again in the presence of multiple-pulse dipolar decoupling. Pairs of experiments are coadded, one with and one without π_z rotation pulse to eliminate spurious transverse magnetization. The π_z rotation was achieved with the pulse sequence $\tau-(\pi/2)_x-\tau-(\pi/2)_y-2\tau-(\pi/2)_y-\tau-(\pi/2)_{-x}-\tau$, which is identical with the first half of a MREV-8 cycle. In addition, simultaneous phase alternation of the detection pulse and of the computer phase eliminates artifacts originating from the multiple-pulse sequence during detection. (b) Selective saturation-transfer experiment. The mixing time τ_m is divided into periods of selective inversion in the presence of multiple-pulse dipolar decoupling and spin-diffusion periods of length τ_{diff}. The measurement is performed as in a. A nonselective π_x prepulse is inserted in every second experiment combined with alternate addition and subtraction of the signals to eliminate the equilibrium magnetization reached for long τ_m values. In both experimental schemes, magic-angle sample spinning is applied for eliminating chemical shielding anisotropy.

(b) Saturation-Transfer Experiment. A saturation-transfer experiment is used to determine the composition of the various phases of an inhomogeneous polymer blend. The experiment is related to the truncated driven NOE experiment used in the liquid phase.[43] By selective irradiation for an extended time, a chosen group of isochronous spins is saturated. At the same time spin diffusion proceeds, leading to saturation of all those spin groups dipole-coupled to the saturated one.

Because the selective irradiation requires the temporal removal of the dipolar interactions and spin diffusion relies on their presence, it is necessary to rapidly alternate between periods of selective spin inversion in the presence of dipolar decoupling and periods of unperturbed spin diffusion where dipolar interactions are retained, as indicated in Figure 1b.

Perturbation by repetitive inversion and spin diffusion occur effectively at the same time, and in the limit of a long saturation time, τ_m, a dynamic equilibrium between saturation, relaxation, and spin diffusion is reached. To eliminate the unessential equilibrium magnetization from the observed signal, we insert in every second scan a nonselective π_x prepulse (see Figure 1b) and subtract the responses from each other. The observed difference magnetization tends toward zero for extended spin-diffusion times τ_m. The decay constant for spins taking part in spin diffusion is given by the combined effects of saturation, relaxation, and spin diffusion while for unper-

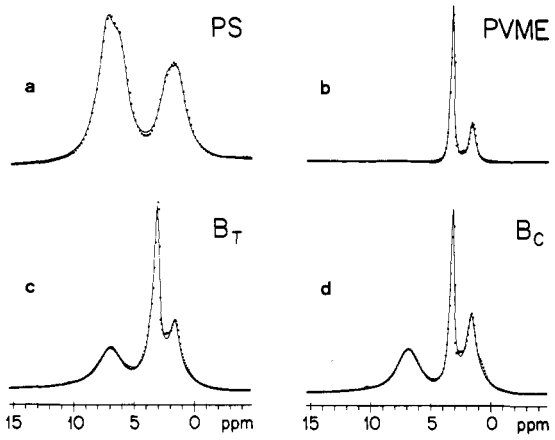

Figure 2. High-resolution proton spectra of (a) polystyrene (PS), (b) poly(vinyl methyl ether) (PVME), (c) blend cast from toluene (B_T) with r = [PS]/[PVME] = 0.80, and (d) blend cast from chloroform (B_C) with r = 1.14. The spectra were obtained at T = 340 K by combining magic-angle sample spinning at 2.5 kHz and MREV-8 multiple-pulse dipolar decoupling. The dots represent the measured signals while the solid curves result from least-square fits. Four Lorentzians were used to fit the PS spectrum, with two lines for the aromatic protons and two lines for the aliphatic protons with relative intensities 3:2:2:1. The spectrum of pure PVME was fitted by three Lorentzians corresponding to the methine, methoxy, and methylene protons with intensity ratios 1:3:2. For the spectral analysis of the polymer blends only four Lorentzians, two for each polymer, were used to avoid highly correlated parameter values.

turbed spins the decay occurs with the longitudinal relaxation time T_1. The different decay constants allow then the separation of the contributions from different phases.

IV. Determination of the Overall Composition of the Blends

A traditional method of determining the composition of polymer blends is the recording of ^1H or ^{13}C NMR solution spectra, which normally allow an easy distinction of the components but with the disadvantage that the possibility of obtaining further information on the morphology of the solid-state sample is lost. A more satisfactory approach to the quantitative analysis is ^{13}C solid-state spectroscopy with magic-angle sample spinning, in which sensitivity enhancement by cross-polarization should be avoided in order to obtain reliable relative intensities.

In the present context, it was convenient to employ high-resolution proton spectroscopy in the solid state. Figure 2 shows the 1D spectra for the two pure homopolymers and for two blends cast from toluene and chloroform, respectively. The spectra were measured at T = 340 K in the presence of magic-angle sample spinning (ν_R = 2.5 kHz) and applying a MREV-8 multiple-pulse sequence. The dots represent experimental points while the solid curves are the results of numerical line shape fits. From the fitted spectral intensities, the molar ratio of the entire sample, r = [PS]/[PVME], is derived, leading to r_{BT} = 0.80 for the blend B_T, and r_{BC} = 1.14 for the blend B_C.

V. Determination of the Spin-Diffusion Rate Constants

The observed spin-diffusion rate constants may be used to derive information on the domain structure of the polymer blends. Although two-dimensional spectra, as demonstrated in ref 26, provide a unique qualitative visualization of the spin-diffusion process, it is often more convenient to apply one-dimensional transient measurements, described in section IIIa, for the quantitative measurement of spin-diffusion rate constants.

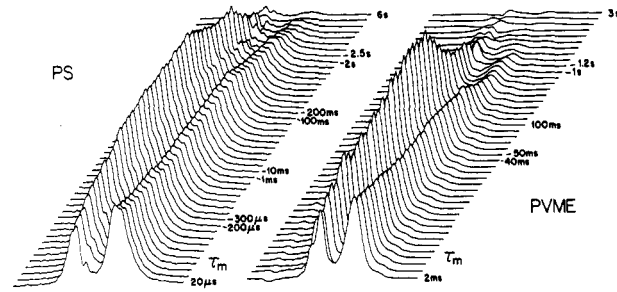

Figure 3. Selective inversion–recovery experiment of Figure 1a applied to pure PS and PVME. The population of the aliphatic spins is selectively inverted and the approach toward internal equilibrium monitored. The spectra obtained from the experiment of Figure 1a were subtracted from the equilibrium spectrum obtained for $\tau_m \gg T_1$. The pulse sequence (c) of Figure 1c in ref 37 was used for the selective inversion with the parameter values N = 5, t_c = 36 μs, ϵ = 27°, n_τ = 3 for PS; and N = 5, t_c = 36 μs, ϵ = 18°, n_τ = 5 for PVME. The time scales are linear between the indicated mixing times.

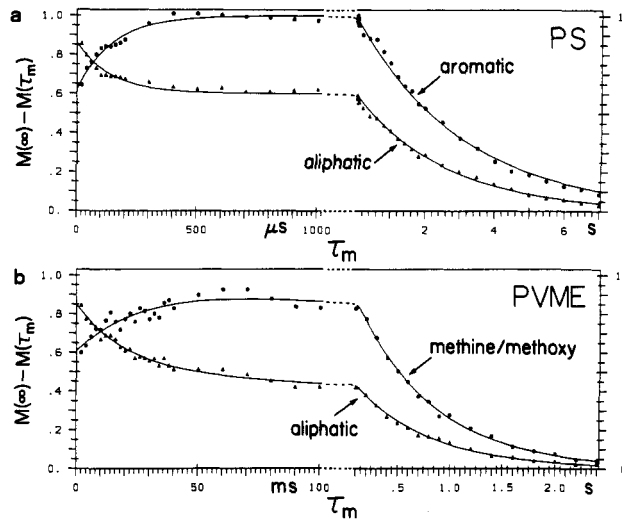

Figure 4. z magnetization for individual lines plotted as a function of the mixing time τ_m by calculating the peak integrals in the selective inversion–recovery spectra shown in Figure 3: (a) pure polystyrene, (b) pure poly(vinyl methyl ether), with initial inversion of the aliphatic lines in both cases. The vertical scale in a and b is chosen such that the magnetization of the aromatic protons, in a, and the magnetization of the methine/methoxy protons, in b, would reach the value 1 for large τ_m and infinitely slow T_1 relaxation. Note the different time scales for a and b and the change of scale in the center of the plot. The solid curves represent a biexponential fit to the experimental data with the parameter values given in the text.

The rate constants for spin diffusion between the two resolved lines within each of the pure polymers PS and PVME were measured with the experiment of Figure 1a. In both cases the aliphatic line was inverted by the initial selective pulse. The results are shown in Figure 3 and 4. The spectra in Figure 3 are obtained by subtracting the spectra for each τ_m value from the equilibrium spectrum which was measured in a separate experiment for $\tau_m \gg T_1$. Figure 4 shows the integrated peak intensities of the individual lines of Figure 3 plotted as functions of the mixing time τ_m. In this representation the τ_m time dependence is similar to that of a diagonal peak (for the irradiated line) or that of a cross peak (for the lines connected by spin diffusion to the irradiated one) in a 2D spin-diffusion spectrum.[26] It should be noted that the "selective" inversion is in practice not fully selective and weakly affects the "unperturbed" lines as well. Their intensity therefore does not start at zero for τ_m = 0. The

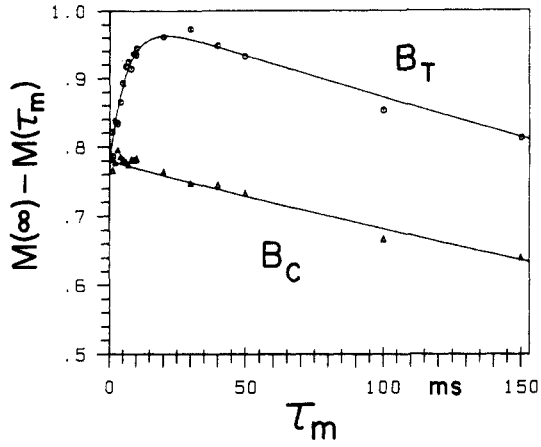

Figure 5. Measurement of the interpolymer spin-diffusion time constant for the blends cast from toluene (B_T) and chloroform (B_C), respectively. The deviation of the methine/methoxy line intensity of PVME from the equilibrium value obtained for $\tau_m \gg T_1$ is plotted in arbitrary units vs. τ_m after selective inversion of the aromatic PS line. The experiment of Figure 1a was used. No spin diffusion is observed in B_C; the decay is entirely due to spin–lattice relaxation (T_1(PVME) = 0.73 s). The initial increase in intensity in B_T is due to interpolymer spin diffusion with a time constant T_{SD}(PS/PVME) = 6.5 ± 0.7 ms. The vertical scale is chosen such that the magnetization for the B_T sample would reach the value 1 for long mixing times and infinitely slow T_1 relaxation. The initial magnetization for the B_C curve, at $\tau_m = 0$, is arbitrarily set to the same value as that for the B_T sample.

solid curves in Figure 4 are the results of a biexponential fit. The fast rate is due to the spin-diffusion process while the slow decay for long mixing times is caused by spin–lattice relaxation. The spin-diffusion rate constants R_{SD} and T_1 values obtained from the fit are R_{SD}(PS) = (144 ± 17)$^{-1}$ μs^{-1} = (7.0 ± 0.8) × 10^3 s^{-1}, T_1(PS) = 2.8 ± 0.2 s, R_{SD}(PVME) = (26 ± 4)$^{-1}$ ms^{-1} = 38 ± 6 s^{-1}, and T_1(PVME) = 0.72 ± 0.02 s.

The comparably slow spin diffusion in PVME indicates high molecular mobility, which partially averages the dipolar interactions, slowing down spin diffusion. This is in agreement with the fact that the measurement temperature of 67 °C is well above the glass transition of PVME at T_g = −30 °C. The spin diffusion in PS, on the other hand, is faster by more than 2 orders of magnitude. The dipolar interactions seem to be preserved, indicating low molecular mobility at the temperature of 67 °C, which is below the corresponding glass-transition temperature T_g = 110 °C.

The rates of spin diffusion between PS and PVME in the blends have been measured by selectively inverting the aromatic peak of PS and subsequently observing the methine/methoxy peak intensity of PVME as a function of the mixing time τ_m. The result of such a measurement for the two blends is displayed in Figure 5. The blend B_T cast from toluene shows a biexponential τ_m dependence. The slow decay is again due to spin-lattice relaxation (T_1(PVME) = 0.73 s) while the fast initial ascent can be attributed to interpolymer spin diffusion in the mixed phase with a rate constant of R_{SD}(PS/PVME) = (6.5 ± 0.7 ms)$^{-1}$ = 154 ± 17 s^{-1}. Spatial spin diffusion between different domains in the sample is expected to lead to a distribution of rate constants. The clear biexponential behavior excludes significant interdomain spin diffusion. This supports the assumed three-phase model where spin diffusion between the two polymers occurs exclusively in the homogeneous mixed domains. Spin diffusion between the two polymers is about 4 times faster than spin diffusion in pure PVME and at least 1 order of magnitude slower than in pure PS. This suggests that the mobility of the PVME chains in the mixed phase is not substantially hindered by the presence of polystyrene. For immobilized PVME chains, faster interpolymer spin diffusion would be expected.

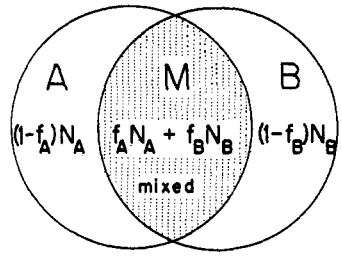

Figure 6. Three-phase model used for a binary mixture of polymers A and B. The mixed phase M contains the fraction f_i of the N_i moles of polymer i (i = A, B). The remaining fractions $(1 - f_i)$ of polymer form the two pure phases. Interpolymer spin diffusion is assumed to take place exclusively in phase M.

In agreement with the earlier 2D measurements, no interpolymer spin diffusion is detected in the blend B_C cast from chloroform. The decay of the PS signal is purely due to spin–lattice relaxation.

A quantitative evaluation of the measured spin-diffusion rates has to be deferred to the future because a strict relation to the domain structure has not yet been established. Although no multiple-pulse dipolar decoupling is applied during the spin-diffusion period τ_m, some partial averaging of the dipolar interaction may be caused by the slow magic-angle sample spinning with $\nu_R \simeq 2.5$ kHz. This rate hardly affects the spin-diffusion rate in rigid polymers like PS with strong dipolar interactions. However, in PVME averaging by molecular motion leads to reduced dipolar couplings which become sensitive to magic-angle sample spinning. This has been confirmed by preliminary measurements. An analysis of these effects is presently in progress.

VI. Determination of the Concentrations within the Three-Phase Model

We denote by f_{PS} and f_{PVME} the fractions of monomer units of PS and PVME, respectively, in the mixed phase M of a polymer blend. The fractions in the two pure phases are then $1 - f_{PS}$ and $1 - f_{PVME}$ (see Figure 6).

For measuring the fraction f_{PVME} in the mixed phase, we saturate selectively the aromatic line of PS with the experimental scheme of Figure 1b. This leads to fast saturation of the mixed-phase contribution of the methine/methoxy line of PVME through spin diffusion, while the signal contribution of the pure PVME phase should remain nearly unperturbed by the saturation. The procedure was applied to both blends by using a spin-diffusion delay of τ_{diff} = 10 ms (see Figure 1b). During this time, the spin diffusion between PS and PVME in the mixed phase of B_T proceeds to near completion.

In Figure 7, parts a and b, the intensity of the methine/methoxy line is plotted as a function of the number n of applied saturation cycles for the two blends B_T and B_C. Examples of spectra leading to the saturation curves in Figure 7 are presented in Figure 8. In contrast to expectations, the entire intensity decays toward zero within a time short compared to T_1. The reason for the fast signal decay becomes clear by inspecting Figure 7c, where the same saturation experiment with irradiation at the resonance frequency of aromatic protons was applied to a sample of pure PVME. The signal also decays rapidly to zero. A fit of the experimental values by an exponential function

$$I_{PVME}(n) = I(0)a^n{}_{PVME} \quad (1)$$

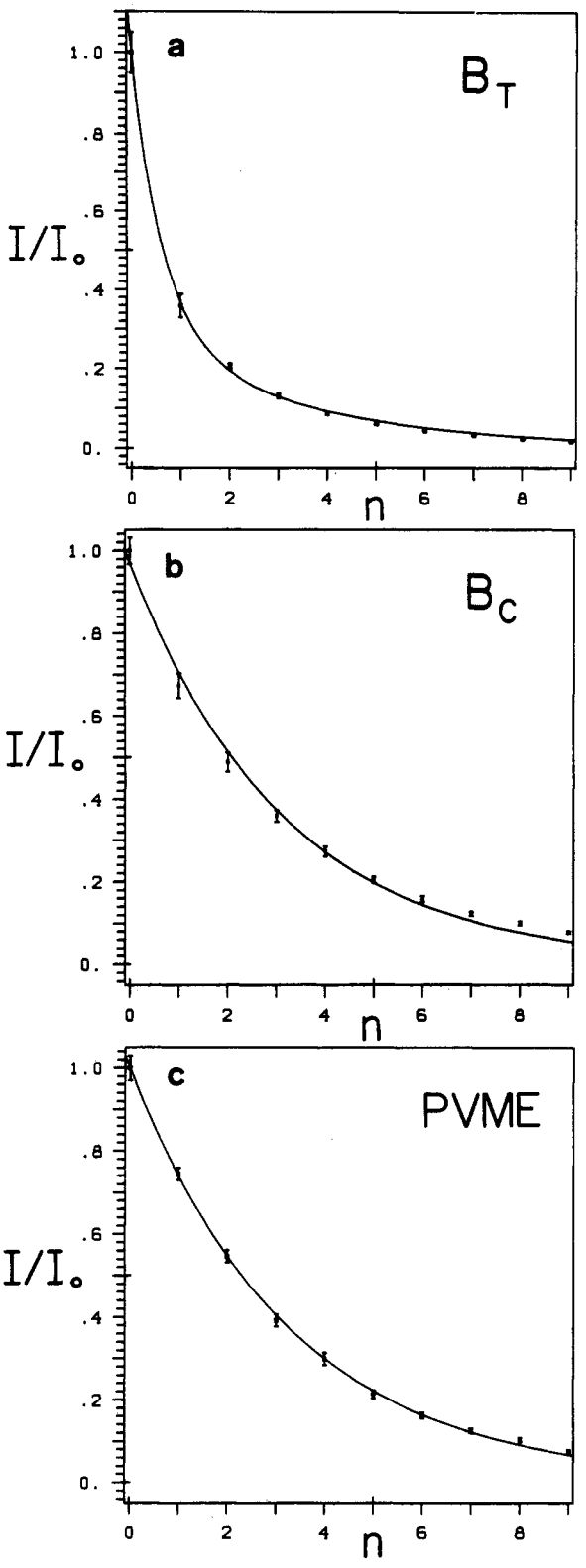

Figure 7. Normalized intensity $I/I(0)$ of the methine/methoxy line of PVME, while saturating at the position of the aromatic PS signal, plotted vs. the number n of saturation cycles in the experiment of Figure 1b with τ_{diff} = 10 ms: (a) Blend cast from toluene (B_T), (b) blend cast from chloroform (B_C), (c) pure PVME sample. The blend B_C and pure PVME show within the experimental error limits the same single-exponential behavior. The blend B_T, in contrast, shows a biexponential decay due to the contributions of the mixed phase and of the pure PVME phase.

produces the values $I(0) = 1.00 \pm 0.01$ and $a_{PVME} = 0.74 \pm 0.01$, implying a decay time constant $T = 33$ ms that is much shorter than the relaxation time $T_1 = 0.725$ s of PVME. This behavior can be interpreted as a direct

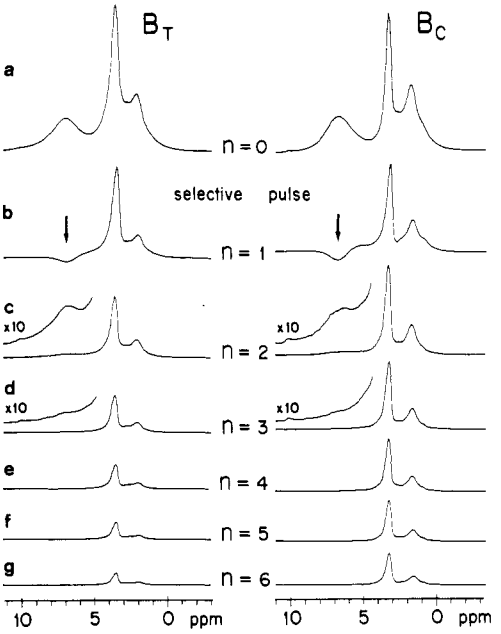

Figure 8. Saturation transfer in the polymer blends B_T and B_C using the experiment of Figure 1b: (a) unperturbed spectra; (b) spectra measured immediately after selective inversion of the aromatic resonance of PS, indicated by arrow; (c) spectra measured after the selective inversion of b followed by a spin-diffusion period τ_{diff} = 10 ms; (d) spectra after two selective inversions and spin-diffusion periods; (e–g) spectra after 3, 4, and 5 selective inversions and spin-diffusion periods. The selective inversion pulse used the parameters $N = 6$, $t_c = 36$ μs, $\epsilon = 27°$, $n_\pi = 5$ (see ref 37).

saturation of the PVME resonances via irradiation of their tails. Each saturation cycle causes an attenuation of the PVME magnetization by a factor a_{PVME}. When interpreting the curves in Figure 7, parts a and b, we have to take into account this direct saturation effect.

The saturation curve of the blend B_C in Figure 7b can be fitted by a single exponential according to eq 1 with the two parameters $I(0) = 0.97 \pm 0.02$ and $a_{PVME} = 0.73 \pm 0.01$. Within experimental error limits, this agrees with the result for the pure PVME sample. There is thus no indication of a mixed phase for the blend cast from chloroform.

The saturation curve of the blend B_T in Figure 7a, on the other hand, requires a biexponential fit

$$I_{PVME}(n) = I(0)[f_{PVME}c^n_{PS\rightarrow PVME} + (1 - f_{PVME})a^n_{PVME}] \quad (2)$$

The first exponential term can be interpreted as arising from the mixed phase where the PVME fraction f_{PVME} is cross-saturated by spin diffusion from PS with the cross-saturation factor $c_{PS\rightarrow PVME}$ (which includes also the effect of direct saturation). The second term with slower saturation, on the other hand, corresponds to the direct saturation of PVME in the pure phase, reducing the magnetization in each cycle by the attenuation factor a_{PVME}. From eq 2 and Figure 7a it is therefore possible to determine the fractional contents of PVME in the different phases. With the value for the attenuation factor from the experiment on pure PVME, $a_{PVME} = 0.74$, the fit delivers the values $I(0) = 1.00 \pm 0.01$, $f_{PVME} = 0.70 \pm 0.02$, and $c_{PS\rightarrow PVME} = 0.20 \pm 0.01$.

To measure f_{PS}, complementary experiments were performed by selectively saturating the methine/methoxy line of PVME and detecting the decay of the aromatic signal. The results are shown in Figure 9, parts a and b for the two blends and in Figure 9c for a sample of pure PS. There is again a direct saturation effect on the aromatic

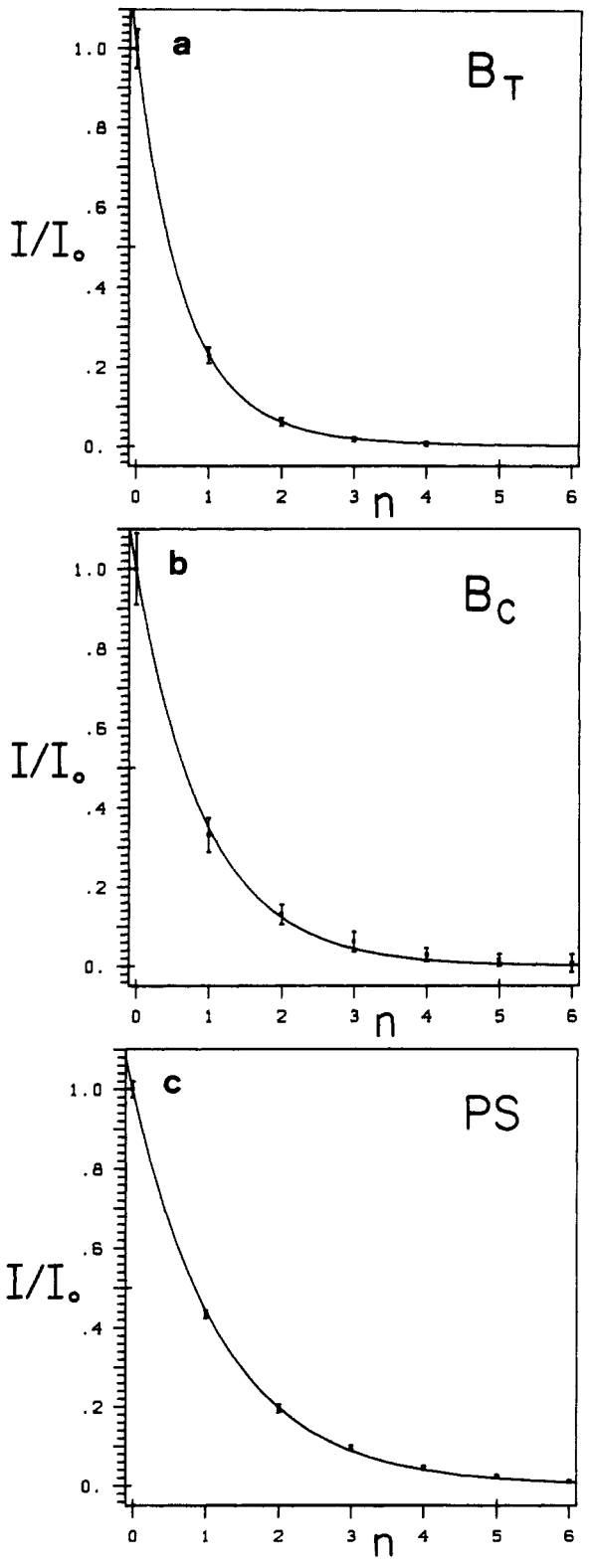

Figure 9. Normalized intensity $I/I(0)$ of the aromatic line of PS, while saturating at the position of the methine/methoxy signal of PVME, plotted vs. the number of saturation cycles n. The experiment of Figure 1b with τ_{diff} = 10 ms was used: (a) blend cast from toluene (B_T), (b) blend cast from chloroform (B_C), (c) pure PS sample. The blend B_C and pure PS show single-exponential behavior. The signal decay of the blend B_T is biexponential due to the contributions of the mixed phase and of the pure PS phase.

signal as put in evidence by the decay of the signal in Figure 9c, which can be fitted by

$$I_{PS}(n) = I(0)a^n_{PS} \quad (3)$$

in analogy to eq 1 with $I(0) = 1.00 \pm 0.01$ and $a_{PS} = 0.44 \pm 0.02$. The direct saturation is here significantly stronger than for the reversed experiment. The decay of the PS signal in the blend B_C in Figure 9b is again exponential with the fit values $I(0) = 1.00 \pm 0.02$ and $a_{PS} = 0.35 \pm 0.06$. Despite the fact that the decay is somewhat faster than for the pure PS sample there is no indication of a significant portion of a mixed phase for the blend B_C cast from chloroform.

The signal decay for the blend B_T of Figure 9a can be fitted biexponentially by

$$I_{PS}(n) = I(0)[f_{PS}c^n_{PVME\rightarrow PS} + (1 - f_{PS})a^n_{PS}] \quad (4)$$

with the values $I(0) = 1.00 \pm 0.02$, $f_{PS} = 0.86 \pm 0.04$, $c_{PVME\rightarrow PS} = 0.195 \pm 0.005$, and $a_{PS} = 0.44$ (assumed). Thus 86% of the PS monomers are contained in the mixed phase M.

Knowledge of $r = 0.80$, $f_{PS} = 0.86$, and $f_{PVME} = 0.70$ in the blend B_T cast from toluene enables one to determine the mole fraction X_{PS} of PS in the mixed phase

$$X_{PX} = rf_{PS}/(rf_{PS} + f_{PVME}) = 1 - X_{PVME} = 0.50 \pm 0.02$$

The fraction f of the total polymer mass contained in the mixed phase is then given by

$$f = \frac{M_{PS}f_{PS}r + M_{PVME}f_{PVME}}{M_{PS}r + M_{PVME}} = 0.79 \pm 0.03$$

where $M_{PS} = 104.1$ g mol^{-1} and $M_{PVME} = 58.1$ g mol^{-1} are the molar weights of the PS and PVME monomer units, respectively.

VII. Summary of the Results on PS/PVME Blends

(i) PS/PVME Blend Cast from Chloroform. In the earlier 2D spin-diffusion studies, no sign of mixed domains could be detected.[26] The selective measurements reported here show no spin diffusion between PS and PVME. It is likely that the sample is composed of extended domains of pure homopolymers with a small, undetectable contact volume between the domains.

(ii) PS/PVME Blend Cast from Toluene. The 2D spin-diffusion study[26] indicated the presence of mixed domains together with pure domains. The interpolymer spin diffusion, measured in this work, can be described, within experimental error limits, by a single exponential. The observed spin-diffusion process is likely due to intimately mixed PS and PVME chains in essentially homogeneous mixed domains. From the spin-diffusion rate it can also be concluded that the mobility of pure PVME is not significantly hindered by the presence of PS chains. The mixed phase contains 79% of the total polymer mass and consists of 64% by weight PS and 36% by weight PVME. The pure PS phase contains 8.5% and the pure PVME phase 12.5% of the total polymer mass.

It should be emphasized that the three-phase model assumed in this paper just serves as a basis for explaining the experimental results. With the information available from the presented NMR measurements it is not possible to further refine this model. Spin diffusion is due to a short-range interaction and conclusions on domain size must be interpreted with care.

Acknowledgment. This research has been supported by the Swiss National Science Foundation. We are grateful to Dr. G. Bodenhausen, Dr. M. H. Levitt, Dr. D. Suter, and Prof. P. Pino for helpful discussions. We thank I. Müller

for her aid in the preparation of this paper.

Registry No. PS (homopolymer), 9003-53-6; PVME (homopolymer), 9003-09-2.

References and Notes

(1) Paul, D. R.; Newman, S. *Polymer Blends*; Academic: New York, 1978; Vol. I and II.
(2) Olabisi, O.; Robeson, L. M.; Shaw, M. T. *Polymer–Polymer Miscibility*; Academic: New York, 1979.
(3) Martuscelli, E., Palumbo, R., Kryszewski, M., Eds. *Polymer Blends: Processing, Morphology and Properties*; Plenum: New York, 1980.
(4) Guinier, A. *X-ray Diffraction in Crystals, Imperfect Crystals and Amorphous Bodies*; Freeman: San Francisco, 1963.
(5) Alexander, L. E. *X-ray Diffraction Methods in Polymer Science*; Wiley: New York, 1969.
(6) Klug, H. P.; Alexander, L. E. *X-ray Diffraction Procedures of Polycrystalline and Amorphous Materials*; Wiley: New York, 1974.
(7) Spuriell, J. E.; Clark, E. S. *Methods Exp. Phys.* **1980**, *16*, 1.
(8) Wang, J.-I.; Harrison, I. R. *Methods Exp. Phys.* **1980**, *16*, 128.
(9) Blazek, A. *Thermal Analysis*; Van Nostrand Reinhold: Princeton, NJ, 1973.
(10) Vadimsky, R. G. *Methods Exp. Phys.* **1980**, *16*, 185.
(11) Nishi, T.; Wang, T. T. *Macromolecules* **1975**, *8*, 909.
(12) de Boer, A.; Challa, G. *Polymer* **1976**, *17*, 633.
(13) Boyer, R. F.; Spencer, R. S. *J. Appl. Phys.* **1944**, *15*, 398.
(14) Bohn, L. *Adv. Chem. Ser.* **1971**, *99*, 66.
(15) Marcincin, K.; Ramanov, A.; Pollak, V. *J. Appl. Polym. Sci.* **1972**, *16*, 2239.
(16) Wetton, R. E.; MacKnight, W. J.; Fried, J. R.; Karasz, F. E. *Macromolecules* **1978**, *11*, 158.
(17) Mehra, U.; Toy, L.; Biliyar, K.; Shen, M. *Adv. Chem. Ser.* **1975**, *142*, 399.
(18) McCall, D. W.; Douglass, D. C. *Polymer* **1963**, *4*, 433.
(19) Douglass, D. C.; Jones, G. P. J. *J. Chem. Phys.* **1966**, *45*, 956.
(20) McBrierty, V. J.; Douglass, D. C.; Kwei, T. K. *Macromolecules* **1978**, *11*, 1265.
(21) McBrierty, V. J. *Faraday Discuss. Chem. Soc.* **1979**, *68*, 78.
(22) Lind, A. C. *J. Chem. Phys.* **1977**, *66*, 3482.
(23) Crist, B.; Peterlin, A. *J. Polym. Sci., Part A-2* **1969**, *7*, 1165.
(24) Douglass, D. C.; McBrierty, V. J. *J. Chem. Phys.* **1971**, *54*, 4085.
(25) Wardell, G. E.; McBrierty, V. J.; Douglass, D. C. *J. Appl. Phys.* **1974**, *45*, 3441.
(26) Caravatti, P.; Neuenschwander, P.; Ernst, R. R. *Macromolecules* **1985**, *18*, 119.
(27) Bank, M.; Leffingwell, J.; Thies, C. *Macromolecules* **1971**, *4*, 43.
(28) Bank, M.; Leffingwell, J.; Thies, C. *J. Polym. Sci.*, Part *A-2* **1972**, *10*, 1097.
(29) Kwei, T. K.; Nishi, T.; Roberts, R. F. *Macromolecules* **1974**, *7*, 667.
(30) Abragm, A. *The Principles of Nuclear Magnetism*, Clarendon Press: Oxford, 1961.
(31) Goldman, M.; Shen, L. *Phys. Rev.* **1966**, *144*, 321.
(32) Cheung, T. T. P.; Gerstein, B. C.; Ryan, L. M.; Taylor, R. E. *J. Chem. Phys.* **1980**, *73*, 6059.
(33) Havens, J. R.; VanderHart, D. L. 25th Experimental NMR Conference, Wilmington, DE, April 1984.
(34) Taylor, R. E.; Pembleton, R. G.; Ryan, L. M.; Gerstein, B. C. *J. Chem. Phys.* **1979**, *71*, 4541.
(35) Ryan, L. M.; Taylor, R. E.; Paff, A. J.; Gerstein, B. C. *J. Chem. Phys.* **1980**, *72*, 508.
(36) Scheler, G.; Haubenreisser, U.; Rosenberger, H. *J. Magn. Reson.* **1981**, *44*, 134.
(37) Caravatti, P.; Levitt, M. H.; Ernst, R. R. *J. Magn. Reson.*, in press.
(38) Forsén, S. H.; Hoffman, R. A. *J. Chem. Phys.* **1963**, *39*, 2892.
(39) Forsén, S. H.; Hoffman, R. A. *J. Chem. Phys.* **1966**, *45*, 2049.
(40) Noggle, J. H.; Schirmer, R. E. *The Nuclear Overhauser Effect, Chemical Applications*; Academic Press: New York, 1971.
(41) Kalk, A.; Berendsen, H. J. C. *J. Magn. Reson.* **1976**, *24*, 343.
(42) Gordon, S. L.; Wüthrich, K. *J. Am. Chem. Soc.* **1978**, *100*, 7094.
(43) Wagner, G.; Wüthrich, K. *J. Magn. Reson.* **1979**, *33*, 675.
(44) Bothner-By, A. A. In *Magnetic Resonance Studies in Biology*; Shulman, R. G., Ed.; Academic: New York, 1979.
(45) Caravatti, P.; Bodenhausen, G. Ernst, R. R. *J. Magn. Reson.* **1983**, *55*, 88.
(46) Rhim, W. K.; Elleman, D. D.; Vaughan, R. W. *J. Chem. Phys.* **1973**, *58*, 1772.
(47) Mansfield, P. *J. Phys. C.* **1971**, *C4*, 1444.

^{13}C NMR Study of the Sequence Distribution of Poly(acrylamide-*co*-sodium acrylates) Prepared in Inverse Microemulsions

Françoise Candau* and Zoubir Zekhnini

Institut Charles Sadron (CRM-EAHP), CNRS-ULP Strasbourg, 67083 Strasbourg Cedex, France

Frank Heatley

Department of Chemistry, University of Manchester, Manchester, M13 9PL, U.K.
Received December 2, 1985

ABSTRACT: The microstructure of poly(acrylamide-*co*-sodium acrylates) of variable compositions and prepared by inverse microemulsion polymerization was studied by ^{13}C NMR. The average copolymer composition is shown to be independent of the degree of conversion, and the sequence monomer distribution analyzed from triad proportions conforms to Bernouillian statistics within experimental error. The reactivity ratios of both monomers are therefore close to unity, a significant difference from the reported literature values obtained for copolymers prepared in solution or inverse emulsion ($r_A \sim 0.3$; $r_M \sim 0.95$). These results confirm a polymerization process by nucleation and interparticular collisions rather than by monomer diffusion through the continuous medium.

Introduction

Over the past 20 years, there have been numerous studies of the influence of the reaction medium on the free-radical copolymerization of acrylamide with ionogenic monomers, e.g., acrylic and methacrylic acids. Two detailed reviews have been published recently.[1,2] Among the factors controlling monomer reactivity are hydrogen bonding, dipolar interactions and electrostatic forces, and EDA complex formation. Consequently, the kinetics of the reaction as well as the microstructure of the resulting

0024-9297/86/2219-1895$01.50/0